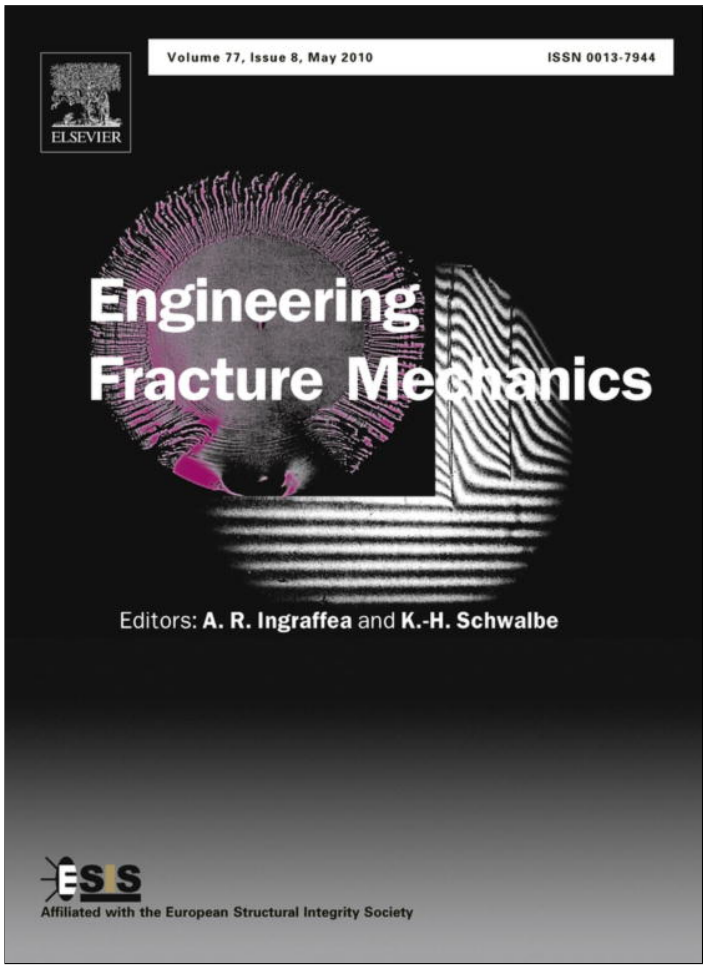

Engineering Fracture Mechanics 77 (2010) 1338–1347

Contents lists available at ScienceDirect

Engineering Fracture Mechanics

journal homepage: www.elsevier.com/locate/engfracmech

Modeling end notched flexure tests to establish cohesive element Mode II fracture parameters

Chien-Chung Chen [a,*], Daniel G. Linzell [b]

[a] Department of Civil and Environmental Engineering, The Pennsylvania State University, State College, PA 16802, USA
[b] Protective Technology Center, The Pennsylvania State University, State College, PA 16802, USA

ARTICLE INFO

Article history:
Received 18 November 2009
Received in revised form 3 March 2010
Accepted 11 March 2010
Available online 15 March 2010

Keywords:
Mode II
Fracture
Polyurea
Steel
Finite element
Cohesive element

ABSTRACT

The objective of this work was to establish Mode II fracture parameters for cohesive elements that can be further utilized to evaluate Mode II interfacial fracture strength of polyurea/AISI 4340 steel composite structures. To obtain the fracture parameters, end notched flexure (ENF) tests were conducted to validate proposed finite element models. The fracture behavior observed from the tests was highly nonlinear and large plastic deformations were involved during crack formation and propagation. A strain incompatibility model was introduced to describe the nonlinearity prior to fracture. This nonlinear and plastic behavior made Linear Elastic Fracture Mechanics (LEFM) approaches not applicable to approximate the fracture parameters. As a result of these experimental observations, finite element analyses of the ENF tests were performed to develop the necessary fracture parameters for cohesive elements selected to replicate the failure modes. Good agreement between the selected numerical models and experimental data was observed.

1. Introduction

Recently, researchers have been seeking and developing new lightweight materials to reinforce existing structures against impact and blast incidents that replace traditional, but heavier materials, such as armor plating. Possessing low density and good energy-absorbing characteristics, polyurea coatings have become potential candidates for retrofitting structures against such extreme events. In addition to its observed advantages under blast loads, polyurea offers other advantages when compared to traditional coatings, including: fast cure time, moisture insensitivity, excellent physical properties, and high abrasion resistance. Many studies have been conducted examining applications of polyurea to wood, masonry, concrete, and steel structures for blast mitigation [1–3]. Since debonding of coating systems can result in undesirable behavior, performance of polyurea coated structural systems, especially under blast loads, is suspected to be dependent on the bond strength between the polyurea and substrate.

In this study, the bond strength between polyurea and a steel substrate was investigated. More specifically, the focus was on using Mode II fracture to characterize shear bond strength of polyurea/steel composite structures. The objective of the study described herein was to develop a numerical model to predict the Mode II bond failure of polyurea bonded to steel so that the resulting model could be used for accurate evaluation and design of polyurea coated steel components and structures.

Fracture strength can be related to the fracture energy and toughness based on basic fracture mechanics theory [4] and can be quantified by experiments. To numerically simulate crack propagation, a numerical model is needed that relates fracture energy and toughness to relevant constitutive relations that can be incorporated into standard finite element codes.

* Corresponding author.
E-mail address: cuc176@gmail.com (C.-C. Chen).

0013-7944/$ - see front matter © 2010 Elsevier Ltd. All rights reserved.
doi:10.1016/j.engfracmech.2010.03.017

Nomenclature

δ	separation in tangential direction
δ_f	failure separation in tangential direction
ε_c	compressive strain
ε_t	tensile strain
ϕ	cross section curvature
a_1	ratio of the distance from the neutral axis to the outer fiber of steel and h
C	resultant of compressive stress
C_1	resultant of compressive stress in the top beam
C_2	resultant of compressive stress in the bottom beam
G_{IIC}	Mode II fracture energy
H	the height of the steel beam
S	maximum shear stress
T	resultant of tensile stress
T_1	resultant of tensile stress in the bottom beam
T_2	resultant of tensile stress in the top beam

In the early 1960s, Dugdale [5] investigated the size of plastic zones in steel sheets containing slits and Barenblatt [6] discussed elastic equilibrium problems of brittle cracks. A cohesive zone modeling technique developed based on the concepts of these two studies has been widely applied to study fracture behavior of various materials [7–16]. Achenbach et al. [7] constructed an analytical model to analyse bond stress and deformation near a crack and established a criterion to describe crack propagation in bonded regions. Later, Ungsuwarungsri and Knauss [8] applied the concept of cohesive zone models to study interfacial bond failure of composites and adhesives. At approximately the same time, Needleman [9,10] introduced a cohesive zone model to study interfacial fracture between a viscoplastic block and a rigid substrate. Later, Ortiz and Blume [11] used the concept of cohesive models to computationally study effects of bond decohesion and sliding on crack tip fields within two linear elastic materials. Recently, Yang et al. [12–15] studied Mode I and Mode II fracture utilizing opening and shear traction–separation laws and extended these models to quantitatively predict crack propagation under mixed-mode conditions for adhesively bonded alloy joints in the bond region. More recently, Li et al. [16] used a cohesive zone model, established by correlating numerical results with experimental data, to predict the Mode I fracture of adhesive joints made of a polypropylene-based composite material.

Results of past studies focusing on cohesive zone model development and the application of these models to bond problems indicate that these techniques can be successfully used to quantitatively predict bond strength and crack propagation in the bonded region and to simulate associated structural responses for various bonded material combinations. Consequently, the cohesive zone approach was applied herein to model the Mode II fracture strength of polyurea bonded steel components, one aspect of a larger study that focused on the blast resistance of polyurea coated steel structural components [17]. The research summarized herein consisted of fracture tests (end notched flexure tests), development and validation of finite element model, and construction of fracture parameters for cohesive elements selected to model the bond failure. Results from ENF tests provided a benchmark to assist with development of these numerical models and construction of fracture parameters for the elements that were selected.

2. Experimental program

ENF tests were carried out to study Mode II fracture behavior of polyurea bonded steel specimens. A summary of the tests that were performed follows. Results from the tests were used to obtain fracture parameters for cohesive elements.

2.1. Selected materials and specimen preparation

ENF test specimens were constructed of two AISI 4340 steel strips (355.6 mm × 25.4 mm × 6.35 mm) bonded by polyurea with one end unbonded as shown in Fig. 1. The dimensions of the ENF test specimens were chosen to match dimensions from

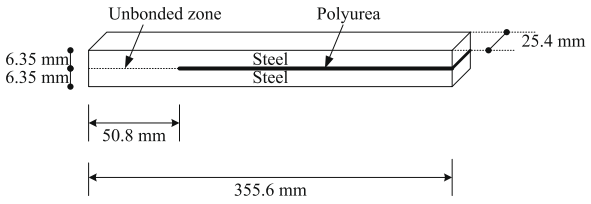

Fig. 1. End notched flexure test specimen.

Table 1
Procedures for ENF specimen preparation.

Steel plates (355.6 mm x 355.6 mm x 6.35 mm) were cut from a steel sheet using waterjet cutting machine.
Surfaces of the plates were degreased and sandblasted.
Polyurea was poured on one plate and brushed evenly over surface with one edge that was covered by a duct tape to create an unbonded zone (50.8 mm wide).
A second steel plate was boned to the first steel plate using polyurea.
The bonded plates were cured at zoom temperature for two weeks.

a companion experimental study of Mode I fracture toughness of polyurea bonded steel members. That study utilized ASTM D3433 [18] to proportion the specimens. Procedures used to prepare the specimens that were tested are listed in Table 1. The polyurea was mixed with 0.127 mm beads as the spacer to control the bond thickness. The finishing polyurea bonded steel plate was then cut into beam specimens using waterjet cutting machine to reduce heat generation caused by cutting. In addition, specimens from plate edges were discarded for quality control.

2.2. Test setup and procedure

The prepared specimens were tested under three-point bending using a 49 kN Universal Testing Machine. A uniformly distributed line load was applied across the center of the beam by a semi-cylindrical bar welded to a loading block that was connected to the testing machine. The test machine was set to displacement control with a loading rate of 0.508 mm/min. Loading was increased continually until bond failure was observed using the recorded load and testing machine crosshead displacement. A total of six specimens were tested. Fig. 2 shows the test setup.

2.3. Test results and their interpretation

Applied force vs. load line displacement diagrams are plotted in Fig. 3. Highly nonlinear and inelastic behavior was observed prior to bond failure. The beginning of this nonlinear behavior was attributed to bond softening between the steel and polyurea, and the later part of the nonlinear behavior was attributed to the combination of bond softening and steel plastic deformation. As observed in Fig. 3, nonlinear behavior became prominent after the applied force exceeded 2 kN, indicating that softening was initiated. Also, the applied forces at failure were above the calculated 3.85 kN yield load for the test specimen, between 4.2 kN and 4.6 kN, indicating that steel yielding occurred before bond failure. The yield load was calculated based on the assumption that the polyurea contribution to the composite section's yield strength was negligible compared to that of the steel section alone. This type of behavior indicated that bond was maintained well into the plastic range for the

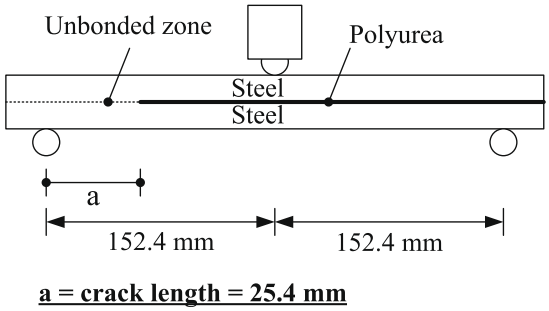

Fig. 2. Schematic of the ENF test setup.

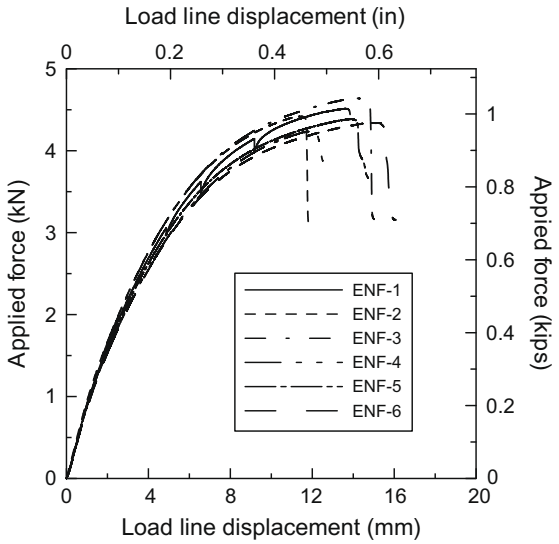

Fig. 3. Applied vs. load line displacement.

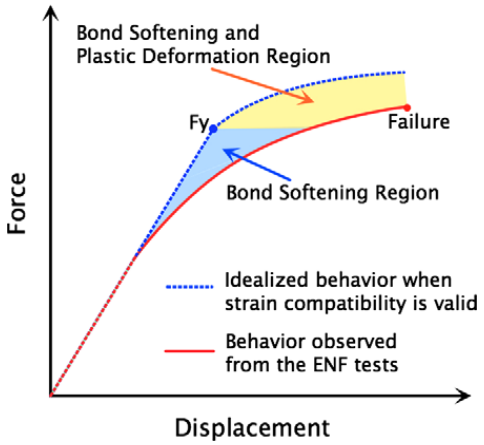

Fig. 4. Schematic description of the nonlinear and inelastic behavior observed from the tests and an ideal load–displacement curve in which softening behavior is absent in the specimen.

specimens that were tested, even bond softening occurred relatively early in each of the tests. Load carrying capacity dropped immediately after the bond failed. The failure occurred at the interface of the polyurea and steel (adhesive failure).

Fig. 4 sketches a typical load–displacement curve observed from the tests superimposed onto an ideal load–displacement curve in which softening behavior is absent in the specimen. It can be seen in Fig. 4 that linearly elastic behavior was not evident prior to reaching F_y and was attributed to deformation along the steel–polyurea interface and, subsequently, strain discontinuity. Fig. 5 details strain profiles that could result for both strain compatibility and strain discontinuity cases. As can be seen in Fig. 5, different strains naturally exist at the interface between the top and bottom steel beams and the polyurea

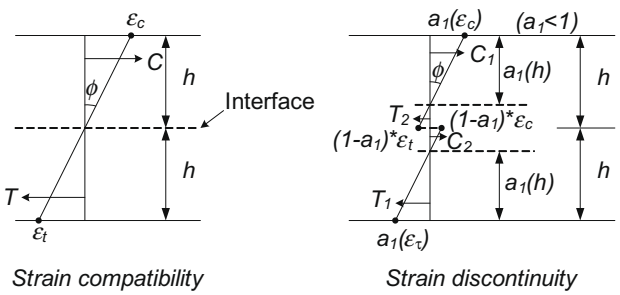

Fig. 5. Strain profiles for the strain compatibility and strain discontinuity cases.

for the strain discontinuity model; tensile strain exists at the bottom surface of the upper steel beam and compressive strain exists at the top surface of the lower steel beam, resulting in new neutral axes in the steel sections.

Strain discontinuity can occur when shear deformation exists in polyurea due to shear forces at the steel and polyurea interfaces. The existence of shear deformation in the polyurea allows for steel deformation at the interface, which are countering the unbalanced shears in the steel sections. To maintain force equilibrium, the shear forces on the top and bottom of polyurea must be equal in magnitude and opposite in direction. Consequently, strain profiles for the top and bottom beams are antisymmetric as shown in Fig. 5.

To show that the observed softening behavior was attributed to shear strain in the polyurea, one can compare moment capacities of a strain compatible section and a strain discontinuity section having the same curvature. Based on the strain profiles (Fig. 5), one can compute the moment capacities of the two sections by applying internal equilibrium (illustrated in Appendix A). The moment capacities for the strain compatibility and discontinuity sections are given in:

$$M_{com} = 1.33Th \tag{1}$$

$$M_{dis} = (2a_1 - 0.67)Th \tag{2}$$

Since a_1 is <1, M_{dis} gives a smaller value than M_{com}. Therefore, an assumed loss of strain compatibility resulted in a decrease in the test specimen's bending capacity, behavior that was observed during the tests. This finding suggests that using a material model that can address the softening behavior is recommended for modeling Mode II interfacial fracture of polyurea coated steel systems.

2.4. Discussion

Critical fracture energy is a material property widely used to identify fracture strength of a material and to predict crack propagation. This fracture energy is generally obtained from fracture tests such as double cantilever beam (DCB) test and ENF test, depending on the nature of fracture. However, experimental measurements of stress, strain and fracture toughness are difficult when plastic deformation exists. As stated earlier, significant plasticity was observed from the ENF tests conducted in this study in both the vicinity of crack tips and in some regions in the steel during Mode II crack formation. Consequently, this highly nonlinear and plastic behavior rendered using LEFM for approximating fracture toughness, and subsequently, the bond strength, inappropriate. As a result, Mode II material parameters were determined by correlating numerical simulations to ENF test results.

3. Numerical program

The objective of the numerical study was to establish fracture parameters that can be used in finite element analyses to predict Mode II interfacial fracture of polyurea coated steel components. This was accomplished using LS-Dyna models of the ENF tests and bond strength was characterized in the models using cohesive elements. As discussed earlier, cohesive zone modeling techniques have been widely used to study interfacial fracture of adhesively bonded structures [9–16]. The past studies indicated that cohesive zone modeling techniques are capable of predicting interfacial bond strength of a broad range of materials. Therefore, the current study applied cohesive elements to model Mode II fracture in the bond region of polyurea bonded steel beams.

3.1. Steel material model and mesh size validation

To develop the necessary cohesive element Mode II fracture properties for polyurea coated steel components, a LS-Dyna model of the ENF specimens was constructed using solid elements to represent the steel with the polyurea bonded zone modeled using the aforementioned cohesive elements. As observed from the tests, the ENF specimens underwent significant plastic deformation before failure. Therefore, a material model that can accurately predict steel inelastic behavior was first needed prior to obtaining bond failure parameters. Therefore, a preliminary numerical study that attempted to simulate inelastic behavior of a single AISI 4340 steel beam under three-point bending test was performed to identify an adequate steel material model. In this preliminary analysis, the mesh size was chosen to be 3.175 mm × 5.08 mm × 0.635 mm. An elasto-plastic material model that incorporated a user-defined flow stress vs. effective plastic strain curve was used for the steel. The stress–strain relation was defined using experimental data from steel tension tests (Fig. 6). Table 2 lists AISI 4340 steel material properties obtained from these tension tests.

Applied force vs. load line displacement (deflection at the midspan) from the numerical simulation was compared with the experimental data as shown in Fig. 7. Good agreement was observed from the comparison, suggesting that the selected material model and mesh size were adequate for the steel for this study.

3.2. Bond modeling

Mat_Coheisve_General (a cohesive material model provided in LS-Dyna [19]) which incorporates a traction–separation law to represent stress–displacement relation for crack evolution was selected to model fracture at the interface of polyurea and

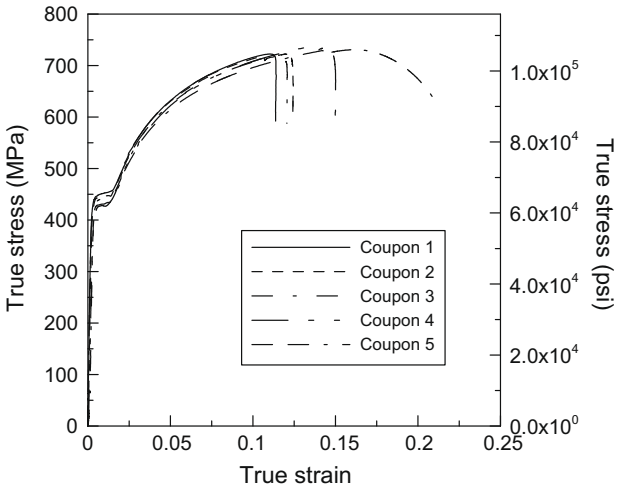

Fig. 6. True stress–strain data from the steel tension tests.

Table 2
AISI 4340 steel material properties obtained from tension tests.

Yield stress (MPa)	Tensile strength (MPa)	Young's modulus (GPa)
442.6	726.6	206.8

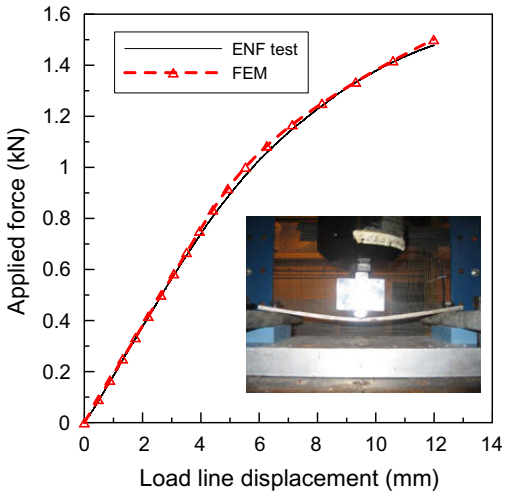

Fig. 7. Comparison of applied force vs. load line displacement data: compare force–displacement data from the steel beam analysis with three-point bending test data (single steel beam).

steel. The stress and displacement defined in the traction–separation law are the bond stress and the relative displacement at the interface, respectively. Fig. 8a shows an arbitrary traction–separation law that can be defined by a user using this material model in LS-Dyna. Bond strength starts to decline when the maximum traction, S, is reached. The area under the traction–separation law represents the critical energy release rate, G_{IIC}. The failure criterion is based on the failure separation, δ_f, which is the tangential relative displacement when bond fails. Debonding is initiated when the tangential opening displacement, δ, of the cohesive elements reaches δ_f. After the failure is initiated no force is required to increase the separation, and the damage process is irreversible. Furthermore, in the cohesive model, the stiffness is reduced by damage when unloading and reloading occur during crack evolution. Unloading and reloading processes follow the path labeled "unloading" as shown in Fig. 8b.

Yang et al. [14] used a trapezoid traction–separation law to simulate elastic–plastic Mode II fracture of adhesively bonded ENF specimens. In their study, fracture parameters were determined by matching numerical simulations with experimental results. It was indicated that the obtained fracture parameters could be used to predict Mode II fracture without further calibrations. Consequently, in the current study, a simplified traction–separation law (trapezoid in Fig. 8b) was used to account

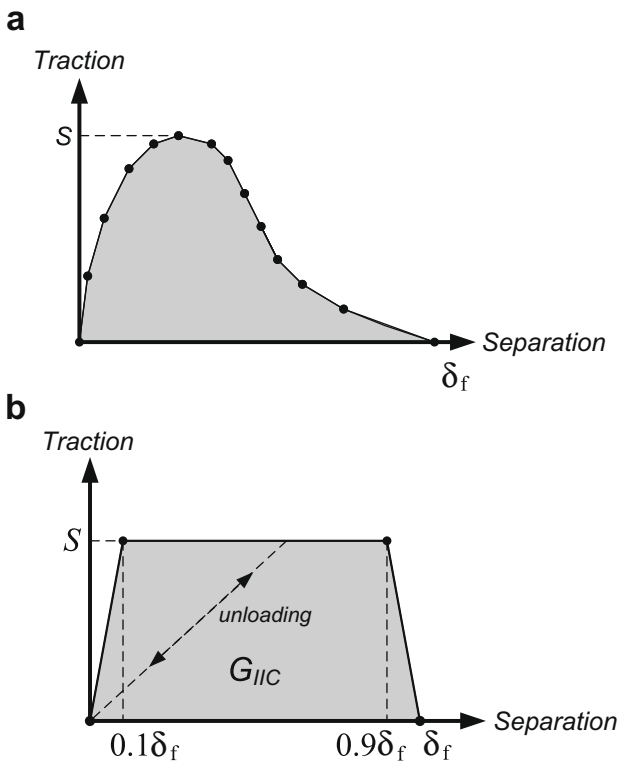

Fig. 8. Traction–separation laws for cohesive elements: (a) an arbitrary traction–separation law that can be defined by users and (b) a simplified traction–separation law that was used for cohesive elements in this study.

for the bond softening behavior using the cohesive elements. In this model, the traction and separation components were used to represent the tangential stress and opening displacements (in the 1 and 2 directions shown in Fig. 9), respectively. The corresponding Mode II material parameter needed to accurately replicate the bond failure, the fracture energy (G_{IIC}) and maximum shear stress (S), were then determined by correlating numerical results with associated experimental data.

3.3. Fracture parameters for cohesive elements

As mentioned earlier, the ENF test specimens underwent a softening behavior before any plastic deformation occurred in the steel. This softening behavior was primarily caused by the decrease in bond strength, which caused deterioration of compatibility between the beam cross sections leading to a reduced moment capacity and increased deformation. Consequently, estimation of the beginning of the bond softening was made by identifying the start of the decline in the beam stiffness from the experimental applied force and displacement curves. As discussed in the previous section, softening behavior became evident after the applied force reached approximately 2 kN. Accordingly, it could be assumed that at 2 kN the shear stress reached its peak and bond softening initiated. Since the bond softening behavior occurred at a relatively early stage during the crack evolution, the maximum shear stress, S, was determined using the assumption that contribution of the thin polyurea layer to any section properties, such as moment of inertia, was negligible. This procedure was utilized to efficiently establish parameters needed for cohesive elements for future computational studies. As the bond line for the tests that were being modeled was located at mid-height of the specimen, it was of interest to determine the shear stress at mid-plane. The calculated shear stress from the tests at the center of the section is 4.65 MPa. Hence, this shear stress was defined as the maximum shear stress, S. With the maximum shear stress determined, the critical Mode II fracture energy was the only variable left to be established for the cohesive elements. The critical Mode II fracture energy was determined using a trial and error method until good agreement was established between the numerical model and experimental results for the ENF

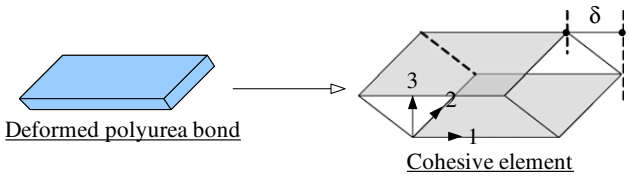

Fig. 9. Bond modeling by cohesive elements.

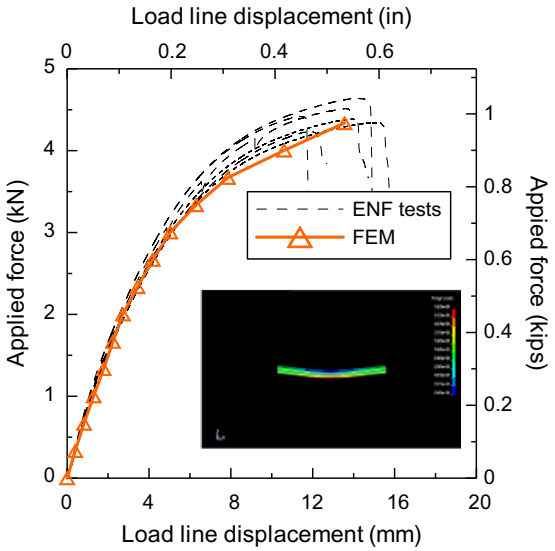

Fig. 10. Comparison of applied force vs. load line displacement data: compare force–displacement data from the ENF test simulation with ENF test data.

tests. From the simulations, the selected fracture energy was 3.5 MPa mm. Results of the analysis are discussed in the following section.

3.4. Results

To evaluate the effectiveness of the cohesive elements, force vs. load line displacement from the ENF test model containing the selected cohesive elements was compared with the experimental results. As can be seen in Fig. 10, the finite element model was able to capture the softening behavior caused by the evolution of interfacial cracks between the polyurea and steel (i.e. bond failure) and was able to accurately predict the strength of the ENF specimen. In addition, shear deformation of the polyurea observed from the tests was also effectively modeled by the numerical simulations, resulting in strain incompatibility at the steel to polyurea interface. Fig. 11 shows the shear deformation observed from the tests and corresponding simulations.

4. Conclusions

In this study, ENF tests were carried out to establish Mode II fracture parameters to predict interfacial fracture of polyurea/steel composite structures. The result of the ENF test showed that bond failure occurred along with significant plastic

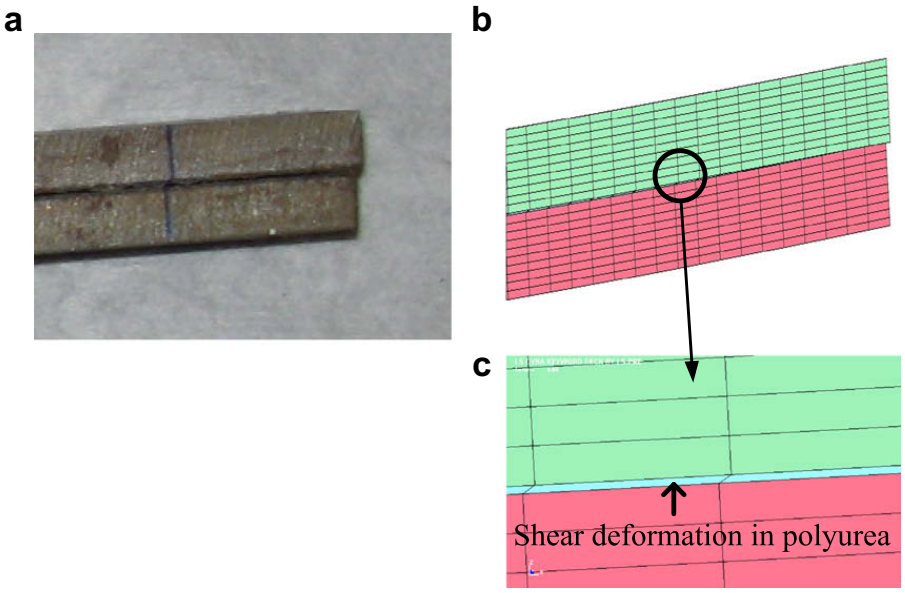

Fig. 11. Shear deformation in polyurea was successfully modeled by the cohesive elements.

deformation in both polyurea and steel, making LEFM not appropriate for approximating fracture properties. Therefore, a finite element model was created to establish necessary fracture parameters to predict the bond strength of polyurea bonded steel structures by correlating numerical simulations with ENF test results. For the numerical simulations, the cohesive zone modeling technique was applied to simulate the Mode II interfacial fracture behavior of polyurea bonded steel specimens. A strength softening model was used for cohesive elements to describe bond softening behavior. From the simulations, fracture parameters for cohesive element models were established. The result of the simulation agreed well with the experimental results. A strain incompatibility caused by shear deformation in polyurea was introduced to describe the nonlinear behavior before steel underwent plastic deformation and this strain incompatibility model was verified by the finite element model. As obtaining fracture parameters with considerable plastic deformation is a challenge, the procedure used to obtain fracture parameters for cohesive elements in this study provides an effective solution to the modeling of ductile bond failures of composite structures.

Acknowledgements

This study is funded by US Office of Naval Research Grant No. ONR N00014-05-1-0844. The authors wish to thank Air Products and Chemicals, Inc. for providing polyurea and manufacturing the specimens used in this study.

Appendix A. Derivation of moments in strain compatibility and strain discontinuity sections

Derivations of formulas to calculate the moment capacities of the two sections presented in Fig. 5 are illustrated below.

A.1. Strain compatibility

For the section with the strain compatibility:
The resultant of the tensile stress:

$$T = \frac{Ebh\varepsilon_t}{2} = \frac{\sigma_t bh}{2} \tag{A1}$$

The resultant of the compressive stress:

$$C = \frac{Ebh\varepsilon_c}{2} = \frac{\sigma_c bh}{2} \tag{A2}$$

b is the width of the specimen. Due to internal equilibrium $T = C$ and $\sigma_t = \sigma_c$. Using internal equilibrium the moment in the section is given by:

$$M_{com} = \left(\frac{\sigma_t bh}{2}\right)\frac{4}{3}h = \frac{2\sigma_t bh^2}{3} = \frac{4}{3}Th \tag{A3}$$

A.2. Strain discontinuity

For the section with strain discontinuity:
The resultant T_1:

$$T_1 = \frac{Eba_1 ha_1\varepsilon_t}{2} = \frac{a_1^2\sigma_t bh}{2} = a_1^2 T \tag{A4}$$

Similarly, for C_1:

$$C_1 = \frac{Eba_1 ha_1\varepsilon_c}{2} = \frac{a_1^2\sigma_c bh}{2} = a_1^2 C = a_1^2 T \tag{A5}$$

and,

$$T_2 = [(1-a_1)\varepsilon_t E](1-a_1)\frac{bh}{2} = (1-a_1)^2 T \tag{A6}$$

C_2 is given by:

$$C_2 = [(1-a_1)\varepsilon_c E](1-a_1)\frac{bh}{2} = (1-a_1)^2 C = (1-a_1)^2 T \tag{A7}$$

Using internal equilibrium the moment in the section is given by:

$$M_{dis} = T_1\left(h - \frac{1}{3}a_1 h\right) + C_1\left(h - \frac{1}{3}a_1 h\right) + T_2\left[\frac{1}{3}(1-a_1)h\right] + C_2\left[\frac{1}{3}(1-a_1)h\right] = \left(2a_1 - \frac{2}{3}\right)Th \tag{A8}$$

Accordingly, a ratio between M_{dis} and M_{com} is obtained:

$$\frac{M_{dis}}{M_{com}} = (1.5a_1 - 0.5) \tag{A9}$$

Eq. (A9) indicates that when a_1 is <1 moments of the section with strain discontinuity are always less than moments of the section with strain compatibility.

References

[1] Porter JR, Dinan RJ, Hammons MI, Knox KJ. Polymer coatings increase blast resistance of existing and temporary structures. AMPTIAC Quart 2002;6:47–52.
[2] Davidson JS, Porter JR, Dinan RJ, Hammons MI, Connell JD. Explosive testing of polymer retrofit masonry walls. J Perf Constr Facil 2004;18(2):100–6.
[3] Chen C, Linzell DG, Long LN, Alpman E. Effectiveness of advanced coating systems for mitigating blast effects on steel components. In: Jones N, Brebbia CA, editors. 10th International conference on structures under shock and impact, 2008 May 14–16; Algarve, Portugal. Southampton (UK): WIT press; 2008. p. 85–94.
[4] Irwin GR. Analysis of stresses and strains near end of crack traversing plate. J Appl Mech 1957;24(3):361–4.
[5] Dugdale DS. Yielding of steel sheets containing slits. J Mech Phys Solids 1960;8:100–4.
[6] Barenblatt GI. The mathematical theory of equilibrium of cracks in brittle fracture. Adv Appl Mech 1962;7:55–129.
[7] Achenbach JD, Keer LM, Khetan RP, Chen SH. Loss of adhesion at the tip of an interface crack. J Elast 1979;9(4):397–424.
[8] Ungsuwarungsri T, Knauss WG. The role of damage-softened material behavior in the fracture of composites and adhesives. Int J Fract 1987;35(3):221–41.
[9] Needleman A. A continuum model for void nucleation by inclusion debonding. J Appl Mech 1987;54(3):525–31.
[10] Needleman A. An analysis of tensile decohesion along an interface. J Mech Phys Solids 1990;38(3):289–324.
[11] Ortiz M, Blume JA. Effect of decohesion and sliding on biomaterial crack-tip fields. Int J Fract 1990;42(2):117–28.
[12] Yang QD, Thouless MD, Ward SW. Numerical simulations of adhesively-bonded beams failing with extensive plastic deformation. J Mech Phys Solids 1999;47(6):1337–53.
[13] Yang QD, Thouless MD, Ward SW. Analysis of the symmetrical 90°-peel test with extensive plastic deformation. J Adhesion 2000;72(2):115–32.
[14] Yang QD, Thouless MD, Ward SW. Elastic–plastic Mode-II fracture of adhesive joints. Int J Solids Struct 2001;38(18):3251–62.
[15] Yang QD, Thouless MD. Mixed-mode fracture analyses of plastically-deforming adhesive joints. Int J Fracture 2001;110(2):175–87.
[16] Li S, Thouless MD, Waas AM, Schroeder JA, Zavattieri PD. Use of Mode-I cohesive-zone models to describe the fracture of an adhesively-bonded polymer–matrix composite. Compos Sci Technol 2005;65(2):281–93.
[17] Chen C. A study of blast effects on polyurea coated steel components. Dissertation. State College (PA): Pennsylvania State University; 2009.
[18] ASTM D3433. 1999. Standard test method for fracture strength in cleavage of adhesives in bonded metal joints. ASTM International.
[19] Livermore Software Technology Corporation. LS-Dyna keyword user's manual. Livermore (CA): The Corporation; 2007.